Theor Chem Account (2008) 120:491–497
DOI 10.1007/s00214-007-0404-5

REGULAR ARTICLE

# The excited states of adenine and thymine nucleoside and nucleotide in aqueous solution: a comparative study by time-dependent DFT calculations

**Roberto Improta · Vincenzo Barone**

Received: 12 November 2007 / Accepted: 9 December 2007 / Published online: 4 January 2008


**Abstract** The effect substitutions at nitrogen atom 1 of thymine and nitrogen atom 9 of adenine have on lowest energy excited electronic states has been studied by means of time-dependent PBE0 calculations in aqueous solution. In agreement with the experimental indications, the vertical excitation energy of the bright state of 1,methyl-thymine, thymine nucleoside and thymine nucleotide is red-shifted with respect to that of thymine. Deoxyribose and deoxyribose-phosphate substituents affect mainly the lowest energy dark state of adenine and thymine, slightly increasing their oscillator strength. The excited states of 9,methyl-adenine and 1,methyl-thymine have also been studied by using the recently developed M052X, CAM-B3LYP and LC-$\omega$PBE density functionals. The computed VEE are in good agreement with those obtained by using PBE0, which, however, provides values closer to the experimental band maximum.

**Keywords** Excited states · Quantum mechanical calculations · Nucleic acids · Time dependent density functional theory

## 1 Introduction

The interaction between UV–visible radiation and nucleic acids, and, thus, the statical and dynamical properties of the excited states of DNA and its constituents (nucleobase, nucleosides and nucleotides) have always been thoroughly studied, due to the potentially dangerous implications for life (photodamage) [1]. This field has been remarkably benefit by the development of ultrafast time-resolved spectroscopical techniques [2–4], which provided fundamental insights into the photodeactivation mechanism of isolated nucleobases [1] and DNA single/double strands [1,5–8]. In this respect, the integration between experiments and computations has also been extremely fruitful [1], allowing for very important advances in the understanding of the intramolecular effects involved in the excited state decay of the insulated pyrimidine [9–17] and purine [19–25] nucleobases.

Experimental results on isolated nucleobases often refer to their nucleoside and nucleotide derivatives. In the former case (see Fig. 1) a ribose/deoxyribose sugar substituent is attached to the nitrogen atom in position 1 (for pyrimidines) or in position 9 (for purines). In the latter case, a phosphoribose substituent is present in the same positions (see Fig. 1). Actually, fluorescence up-conversion time-resolved experiments show that, although the excited state behavior of thymine, thymidine, and thymidine-5′-monophosphate is similar, the addition of sugar, and, especially, of a sugar-phosphate moiety slows down the excited state decay [27]. An analogous study on adenine derivatives shows more striking differences. The fluorescence decay can be described by bi-exponential curves, accounting for a fast and a slow component [28]. Both components are considerably faster for 2′deoxyadenosine and 2′deoxyadeonosine-5′-monophosphate than for adenine. Studying how the substituents on the photoactive moiety of DNA building blocks affect their excited state dynamics is thus important, not only for a more direct comparison with experiments but also for a deeper understanding of the excited state behavior of nucleic acids single and double strands where a phosphoribose backbone is obviously present.

Most of the computational studies in the literature have been performed on the simplest purine and pyrimidine

Contribution to the Nino Russo Special Issue.

R. Improta (✉) · V. Barone
Dipartimento di Chimica, Università Federico II,
Complesso Monte S. Angelo, via Cintia, 80126 Napoli, Italy
e-mail: robimp@unina.it

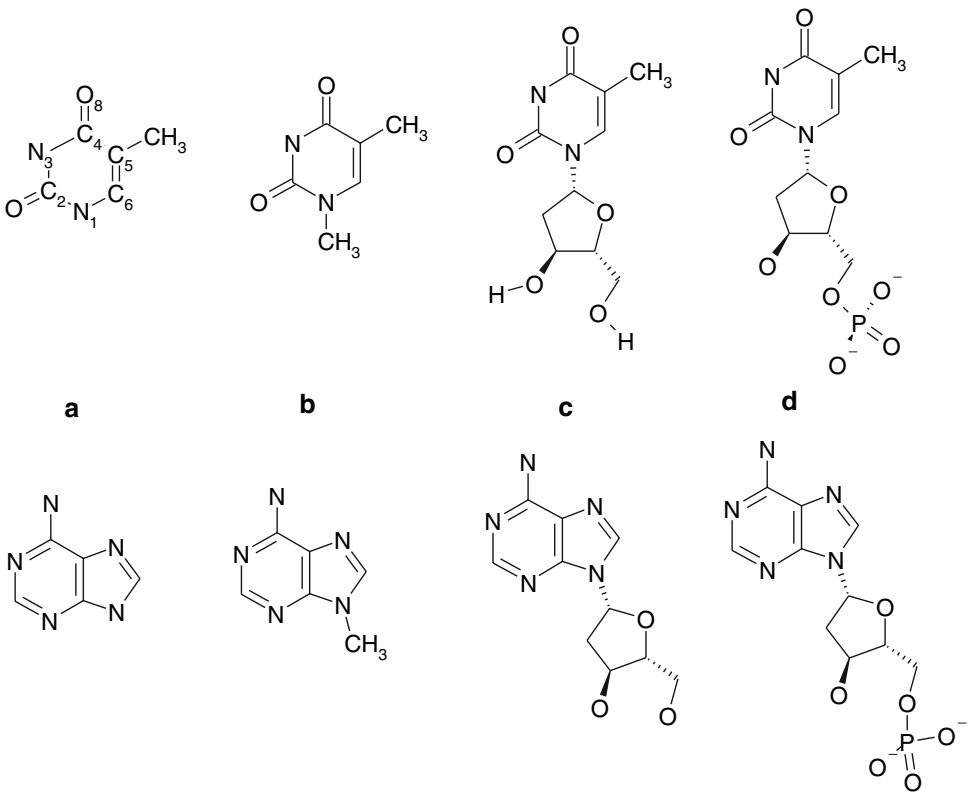


**Fig. 1** Schematic drawings of the systems examined in the present study. *Upper line* **a** thymine (Thy); **b** 1,methyl-thymine (1Me-Thy); **c** deoxy-thymidine (d*T*) **d** deoxy-thymidine-5′-monophosphate (TMP). *Bottom line* **a** 9H-adenine (Ade); **b**; 9,methyl-adenine (9Me-Ade); **c** 2′deoxyadenosine (d*A*); **d** 2′deoxyadeonosine-5′-monophosphate (AMP)

parent compounds of the nucleobases: adenine, guanine, thymine/uracil, cytosine [9–25]. The only exceptions are two very recent computational studies of methyl-adenine [29] and 9-methyl-guanine [30] and, especially, an interesting study of DNA and RNA nucleosides [31]. However, this latter study has been performed in the gas phase, whereas solvent effects significantly modulate the relative stability of the lowest energy excited states of nucleobases [9–13]. Furthermore, to the best of our knowledge, the effect of the strongly charged phosphate dianion on nucleotide's excited states has never been investigated until now.

The present paper is thus devoted to explore how the nature of the substitution at position 1 of pyrimidine and 9 of purine modulates the absorption spectra of nucleobases. To this aim, for what concerns pyrimidine, we have studied in aqueous solution the lowest energy excited electronic states of thymine (Thy), 1,methyl-thymine (1Me-Thy), deoxy-thymidine (d*T*), deoxy-thymidine-5′-monophosphate (TMP). For what concerns purines we have instead studied in aqueous solution the lowest energy excited states of 9H-adenine (Ade), 9,methyl-adenine (9Me-Ade), 2′deoxyadenosine (dA) and 2′deoxyadeonosine-5′-monophosphate (AMP).

Ground-state calculations will be performed at the density functional level (DFT), while the excited states will be studied at the time-dependent (TD) DFT level. We choose the hybrid PBE0 functional [32] as reference functional, since, despite the absence of adjustable parameters, it provides a reliable description of conformational equilibria [33–39] and excited state properties in biological systems[40–43]. In particular, it has already shown very good performances when applied to the study of nucleobases [9–13,29].

However, PBE0 could be plagued by the well-known failures of DFT and TD-DFT calculations when describing dispersion interactions and electronic transitions with significant charge transfer (CT) character [44–51]. This could be a serious drawback when studying single/double strand DNA oligomers, where both experiments and computations indicate the possible involvement of CT transitions [1,5,29].

It would thus desirable check how some new density functionals, which have been tailored to avoid the aforementioned drawbacks, [52–55] describe the excited state behavior of nucleic acids. As a first step in this direction, we compared the PBE0 results for 9Me-Ade and 1Me-Thy with those delivered by three additional density functionals, i.e. CAM-B3LYP [56], LC-$\omega$PBE [57], and M052X [58].

## 2 Computational details

Ground-state geometry optimizations have been performed at the PBE0/6-31$G(d)$ level. PBE0 [32] is an hybrid functional in which the spurious self-interaction is partly cured by mixing PBE and Hartree–Fock exchange with amounts determined in order to fulfill a number of physical conditions,

without resorting to any fitting procedure [32]. PBE0 obeys indeed both the Levy condition [59] and the Lieb–Oxford bound [60], providing a fairly accurate description of the low density/high-gradient regions. Excited state vertical excitation energies (VEE) have been computed at the TD-PBE0 [40] level, by using standard 6-31$G(d)$, 6-31+$G(d, p)$, and 6-311+$G(2d, 2p)$ basis sets.

We also checked the performance of two recently developed density functionals, specifically designed for a suitable treatment of long-range charge transfer transitions, i.e. LC-$\omega$PBE [57] and CAM-B3LYP [56]. LC-$\omega$PBE [57] has been built starting from the PBE exchange functional, introducing range separation into the exchange component and replacing the long-range portion of the approximate exchange by its Hartree–Fock counterpart. CAM-B3LYP [56] combines the hybrid qualities of B3LYP and the long-range correction proposed by Hirao et coll [61]. Finally, we performed test calculations by using M052X [58], which is based on simultaneously optimized exchange and correlation functionals both including kinetic energy density and has shown very good performance in the treatment of dispersion interactions in non-covalent complexes.

Bulk solvent effects have been included by means of the polarizable continuum model (PCM) [62–64]. Actually, our previous computational studies [9–13] indicate that including the solvent molecules of the first solvation shell is very important to get an accurate estimate of the relative energy of the nucleobases' lowest energy excited states in water solution. The presence of explicit solute–solvent hydrogen bonds is particularly important for the excited states with $n \rightarrow \pi^*$ character, which are destabilized by $\approx$0.2 eV with respect the $\pi \rightarrow \pi^*$ excited states. However, since the present paper is mainly devoted to the study of substituent effects, we shall consider bulk solvent effect only.

All the calculations have been performed by using a development version of the Gaussian package [65].

## 3 Results

### 3.1 Thymine derivatives

PBE0 calculations predict that, independently of the nature of the N1 substituent, the two lowest energy transitions fall at $\approx$5 eV (see Table 1) [9–13] and exhibit different features. Confirming previous computational analysis, one state (hereafter Sn) is almost dark and has a predominant n/$\pi^*$ character, involving the transfer of an electron from a Kohn–Sham (KS) orbital mainly corresponding to the Lone Pair of the C4-O8 carbonyl group (hereafter $n$) toward a $\pi^*$ orbital of the ring (hereafter $\pi^*$). For thymine this transition mainly corresponds to a HOMO-1→LUMO excitation. The other one (hereafter S$\pi$) is bright and it has $\pi/\pi^*$ character, since

**Table 1** Vertical excitation energies (in eV) computed for different thymine derivatives in aqueous solution according to PCM/TD-PBE0 excited state calculations on geometries provided by PCM/PBE0/6-31$G(d)$ optimizations

| | Thy | 1Me-Thy | d$T$ | TMP |
|---|---|---|---|---|
| 6-31$G(d)$ | | | | |
| S$n$ | 5.13 (0.00) | 5.12 (0.00) | 5.15 (0.07) | 5.13 (0.04) |
| S$\pi$ | 5.22 (0.18) | 5.12 (0.22) | 5.07 (0.19) | 5.02 (0.20) |
| 6-31+$G(d, p)$ | | | | |
| S$n$ | 5.18 (0.00) | 5.18 (0.00) | 5.17 (0.001) | 5.16 (0.001) |
| S$\pi$ | 5.06 (0.21) | 4.94 (0.26) | 4.93 (0.27) | 4.87 (0.27) |
| 6-311+$G(2d, 2p)$ | | | | |
| S$n$ | 5.16 (0.00) | 5.15 (0.00) | 5.14 (0.001) | 5.14 (0.001) |
| S$\pi$ | 4.99 (0.20) | 4.86 (0.24) | 4.87 (0.26) | 4.82 (0.26) |

Notes: Experimental band maxima: Thy 4.68 eV [10]; 1Me-Thy 4.55 eV; d$T$ 4.64 eV [66]; TMP 4.64 eV [66]
Oscillator strengths are given in parentheses

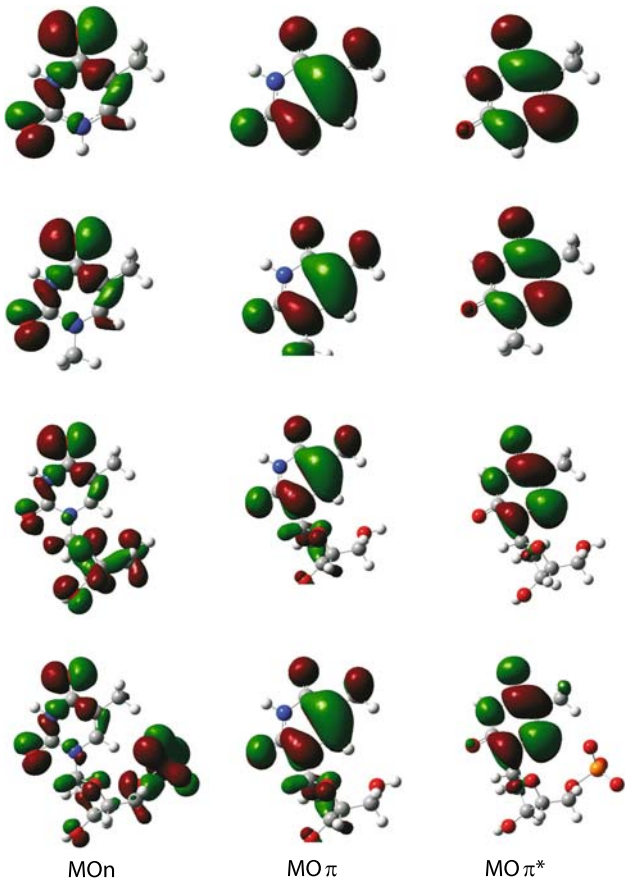


**Fig. 2** Schematic picture of the KS orbitals involved in the SN and S$\pi$ transitions in thymine derivatives, from the *top*: thymine (Thy); 1,methyl-thymine (1Me-Thy); deoxy-thymidine (d$T$); deoxy-thymidine-5′-monophosphate (TMP)

can be described as an excitation from the highest energy $\pi$ orbital of the ring (hereafter $\pi$) to $\pi^*$. In thymine this transition corresponds to the HOMO→LUMO excitation.

A schematic picture of the above orbitals can be found in Fig. 2.

In 1Me-Thy methyl substitution on N1 does not affect significantly n and $\pi^*$ orbitals, whereas the $\pi$ orbital is slightly destabilized because of an anti-bonding interaction with the CH bonds of the methyl group. As a consequence the S$\pi$ transition is red-shifted by $\approx$0.1 eV with respect to thymine, in agreement with the experimental indications [10,66]. Furthermore the relative stability of S$\pi$ with respect to Sn increases.

When a deoxyribose or a phosphoribose substituent is present on N1, $\pi$ and $\pi^*$ orbitals are not significantly changed with respect to 1Me-Thy. The S$\pi$ transition energy indeed is only slightly affected, as indicated by the experimental spectra too [66].

The $n$ orbital is instead strongly mixed with the orbital localized on the ribose or on the phosphoribose moiety, and thus in the Sn transition there are noticeable contributions from the ribose orbitals. As a consequence, although the transition energy does not significantly changes, this transition acquires some oscillator strength. On the other hand, Sn is always much weaker than S$\pi$, except when the smallest 6-31$G(d)$ basis set is used, which is not adequate to treat d$T$ and, especially, dianionic species like TMP. Furthermore, the amount of phosphoribose$\rightarrow$thymine charge transfer involved in the $S_n$ transition is negligible, suggesting that the presence of ribose affects the description of the transition in terms of excitation between KS orbitals, but does not change its main physical features. According to TD-PBE0 calculations the S$\pi$ state corresponds to the third excited state, whereas the two lowest energy states correspond to phosphate$\rightarrow$pyrimidine CT transitions. However, this result has to be considered with a lot of caution. Indeed, the energy of CT transitions involving KS orbitals with vanishingly small overlap could be underestimated by the PBE0 functional [46]. Furthermore, the standard implementation of PCM/TD-DFT, based on the Linear Response theory [64], could be not fully adequate to treat solvent effects on electronic transitions involving very large dipole moment shifts [67,68].

In agreement with experiments, PBE0 calculations thus provide very close excitation energies for 1Me-Thy, d$T$, and TMP. It is indeed important to remind that the shape of the absorption spectra is significantly affected by the vibrational degrees of freedom [69–71] and, thus, the comparison between computed VEE and absorption maxima can give only semi-quantitative indications.

### 3.2 Adenine derivatives

In agreement with previous CASPT2 studies on adenine [24–26], three electronic transitions contribute to the lowest energy absorption band, two with $\pi/\pi^*$ character (usually labeled $\pi^*L_a$ and $\pi^*L_b$, respectively, hereafter simply $L_a$ and $L_b$) and one with $n/\pi^*$ character (hereafter, Sn). Most of the absorption intensity is carried by the spectroscopic $L_a$ state, which corresponds essentially to the transition from the highest energy $\pi$ occupied molecular orbital (hereafter $\pi$) to the lowest energy $\pi^*$ molecular orbital (hereafter $\pi^*$) (see Fig. 3). For adenine those orbitals actually correspond to the HOMO and the LUMO, respectively. In contrast, the $L_b$ state corresponds mainly to an HOMO$\rightarrow$LUMO+1 transition. Finally, the Sn transition involves the transfer of an electron from a non-bonding KS orbital ($n$ in Fig. 3) to the $\pi^*$ orbital. For adenine, it corresponds to an HOMO-1$\rightarrow$LUMO transition.

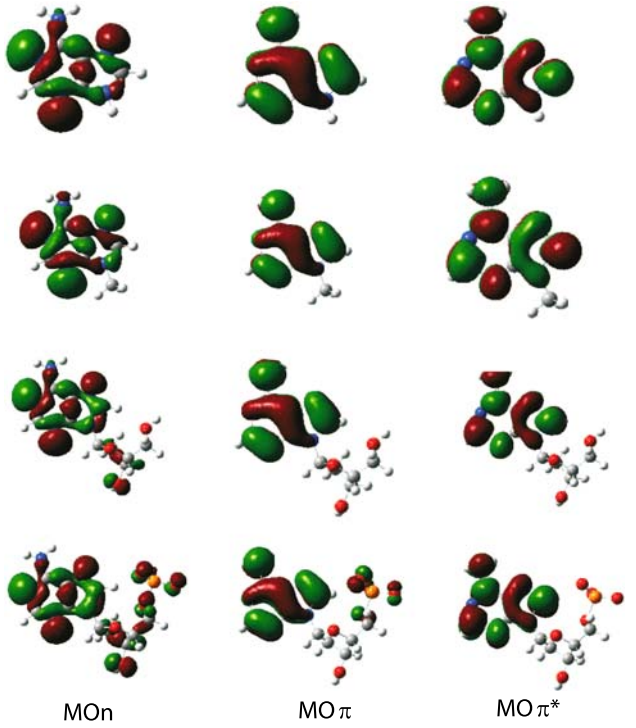


**Fig. 3** Schematic picture of the KS orbitals involved in the SN and S$\pi$ transitions in adenine derivatives, from the *top*: 9H-adenine (Ade); 9,methyl-adenine (9Me-Ade); 2′deoxyadenosine (dA); 2′deoxyadeonosine-5′-monophosphate (AMP)

The interaction between the methyl group on nitrogen atom 9 and the $\pi$ orbital is weaker than the corresponding interaction involving the methyl group on N1 in pyrimidine (see Fig. 3). As a consequence, the transition energy to the $L_a$ excited state does not significantly change when going from Ade to AMP, all the VEEs falling in a range of 0.05 eV (see Table 2).

Ribose and phosphoribose substituents affect mainly the Sn state, because of the mixing between $n$ and some KS orbitals mainly localized on the ribose ring, although the mixing is smaller than that occurring in thymine derivatives. Also in this case the most remarkable effect concerns an increase of the Sn oscillator strength, whereas the energy of the transition does not significantly change with respect to

**Table 2** Vertical excitation energies (in eV) computed for different adenine derivatives in aqueous solution according to PCM/TD-PBE0 excited state calculations on geometries provided by PCM/PBE0/6-31$G(d)$ optimizations

| | Ade | 9Me-Ade | d$A$ | AMP |
|---|---|---|---|---|
| 6-31$G(d)$ | | | | |
| S$n$ | 5.35 (0.001) | 5.34 (0.001) | 5.33 (0.001) | 5.34 (0.03) |
| $L_a$ | 5.24 (0.26) | 5.19 (0.24) | 5.17 (0.28) | 5.18 (0.26) |
| $L_b$ | 5.44 (0.07) | 5.40 (0.09) | 5.41 (0.10) | 5.38 (0.09) |
| 6-31+$G(d, p)$ | | | | |
| S$n$ | 5.36 (0.001) | 5.34 (0.001) | 5.34 (0.012) | 5.35 (0.005) |
| $L_a$ | 5.10 (0.31) | 5.05 (0.30) | 5.04 (0.34) | 5.05 (0.35) |
| $L_b$ | 5.33 (0.05) | 5.30 (0.06) | 5.29 (0.06) | 5.27 (0.07) |
| 6-311+$G(2d, 2p)$ | | | | |
| S$n$ | 5.34 (0.001) | 5.33 (0.00) | 5.32 (0.006) | 5.33 (0.004) |
| $L_a$ | 5.05 (0.31) | 4.98 (0.30) | 4.99 (0.33) | 5.00 (0.35) |
| $L_b$ | 5.28 (0.05) | 5.26 (0.04) | 5.25 (0.06) | 5.23 (0.06) |

Notes: experimental band maximum: d$A$ 4.77 eV [66]; AMP 4.77 eV [66]
Oscillator strengths are given in parentheses

that found in 9Me-Ade. Finally, as already found for TMP, TD-PBE0 calculations predict the existence of two low-lying phosphate→purine CT transitions, corresponding to the first and the third excited states, respectively.

### 3.3 Comparison among different density functionals

As a first step, we have computed the VEE of 1Me-Thy by using, for all the TD-DFT calculations, the ground-state equilibrium geometry optimized at the PBE0/6-31$G(d)$ level (see Table 3). All the density functionals employed provide a similar description of the KS orbitals involved in the two lowest

**Table 3** Vertical excitation energies (in eV) computed for 1Me-Thy derivatives in aqueous solution according to PCM/TD-DFT calculations employing different density functionals on geometries computed at the PCM/PBE0/6-31$G(d)$ level

| | PBE0 | LC-$\omega$PBE | CAM-B3LYP | M052X |
|---|---|---|---|---|
| 6-31$G(d)$ | | | | |
| S$n$ | 5.14 (0.00) | 5.32 (0.00) | 5.37 (0.00) | 5.29 (0.00) |
| S$\pi$ | 5.13 (0.22) | 5.26 (0.27) | 5.27 (0.27) | 5.36 (0.29) |
| 6-31+$G(d, p)$ | | | | |
| S$n$ | 5.19 (0.00) | 5.38 (0.00) | 5.44 (0.00) | 5.38 (0.00) |
| S$\pi$ | 4.95 (0.26) | 5.07 (0.30) | 5.07 (0.30) | 5.18 (0.31) |
| 6-311+$G(2d, 2p)$ | | | | |
| S$n$ | 5.15 (0.00) | 5.36 (0.00) | 5.41 (0.00) | 5.38 (0.00) |
| S$\pi$ | 4.86 (0.24) | 4.98 (0.28) | 4.99 (0.28) | 5.09 (0.29) |

Notes: Experimental band maxima: 1Me-Thy 4.55 eV [10]
Oscillator strengths are given in parentheses

**Table 4** Vertical excitation energies (in eV) computed for 1Me-Thy derivatives in aqueous solution according to PCM/TD-DFT calculations employing different density functionals

| | PBE0 | LC-$\omega$PBE | CAM-B3LYP | M052X |
|---|---|---|---|---|
| 6-31$G(d)$ | | | | |
| S$n$ | 5.14 (0.00) | 5.33 (0.00) | 5.36 (0.00) | 5.29 (0.00) |
| S$\pi$ | 5.13 (0.22) | 5.30 (0.27) | 5.30 (0.26) | 5.38 (0.28) |
| 6-31+$G(d, p)$ | | | | |
| S$n$ | 5.19 (0.00) | 5.39 (0.00) | 5.43 (0.00) | 5.37 (0.00) |
| S$\pi$ | 4.95 (0.26) | 5.11 (0.30) | 5.09 (0.29) | 5.20 (0.31) |
| 6-311+$G(2d, 2p)$ | | | | |
| S$n$ | 5.15 (0.00) | 5.37 (0.00) | 5.41 (0.00) | 5.37 (0.00) |
| S$\pi$ | 4.86 (0.24) | 5.02 (0.27) | 5.01 (0.27) | 5.12 (0.29) |

The geometry optimized by each of the functionals (by using the 6-31$G(d)$ basis set) is used in the TD-DFT calculation. Oscillator strengths are given in parentheses

energy electronic transitions. Furthermore, Sn and S$\pi$ states have similar VEEs and the relative stability of the latter state strongly increases by using larger basis sets. From a quantitative point of view, the VEE's computed at the LC-$\omega$PBE or CAM-B3LYP level are larger by $\approx$ 0.1 eV and those at the M052X level by $\approx$ 0.2 eV than the PBE0 results. This latter functional thus provides a VEE closer to the experimental band maximum. PBE0 and M052X predict that the energy difference between Sn and S$\pi$ states is smaller than that provided by CAM-B3LYP and LC-$\omega$PBE calculations. However, when the largest basis set is used, all the density functionals indicate that the S$\pi$ state corresponds to the lowest energy excited state.

The geometries predicted by the three density functionals examined are very similar to that obtained at the PBE0 level. Indeed, as shown in Table 4, when the geometry optimized by each of the functionals (instead of the PBE0 one) is used in the TD-DFT calculations, the VEEs do not significantly change, the differences being always smaller than 0.04 eV.

The above considerations hold also for 9Me-Ade. All the density functionals provide the same energy ordering among the S$n$, $L_a$ and $L_b$ excited states (see Table 5). However, when compared to the TD/PBE0 results, the VEE of the bright $L_a$ state is overestimated by $\approx$0.3 eV by TD/M052X and TD/LC$\omega$PBE calculations, and by $\approx$0.2 eV by TD/CAM-B3LYP calculation. Comparison between Tables 5 and 6 indicates that the differences among the equilibrium geometry provided by the studied functionals have a limited impact on the computed VEE.

## 4 Concluding remarks

We have studied how the nature of the substituents on N1 (in thymine) or N9 (in adenine) affects the vertical excita-

**Table 5** Vertical excitation energies (in eV) computed for 9Me-Ade adenine derivatives in aqueous solution according to PCM/TD-DFT calculations employing different density functionals on geometries computed at the PCM/PBE0/6-31$G(d)$ level

| | PBE0 | LC-$\omega$PBE | CAM-B3LYP | M052X |
|---|---|---|---|---|
| 6-31$G(d)$ | | | | |
| S$n$ | 5.35 (0.00) | 5.48 (0.13) | 5.61 (0.00) | 5.68 (0.00) |
| $L_a$ | 5.18 (0.26) | 5.50 (0.26) | 5.40 (0.34) | 5.50 (0.38) |
| $L_b$ | 5.43 (0.07) | 5.53 (0.02) | 5.52 (0.04) | 5.66 (0.03) |
| 6-31+$G(d, p)$ | | | | |
| S$n$ | 5.35 (0.00) | 5.53 (0.00) | 5.63 (0.00) | 5.70 (0.00) |
| $L_a$ | 5.04 (0.31) | 5.32 (0.40) | 5.22 (0.38) | 5.34 (0.41) |
| $L_b$ | 5.32 (0.05) | 5.47 (0.03) | 5.43 (0.02) | 5.58 (0.03) |
| 6-311+$G(2d, 2p)$ | | | | |
| S$n$ | 5.33 (0.00) | 5.51 (0.00) | 5.61 (0.00) | 5.70 (0.00) |
| $L_a$ | 4.98 (0.30) | 5.26 (0.38) | 5.16 (0.37) | 5.28 (0.40) |
| $L_b$ | 5.26 (0.04) | 5.40 (0.03) | 5.36 (0.02) | 5.52 (0.03) |

Oscillator strengths are given in parentheses

**Table 6** Vertical excitation energies (in eV) computed for 9Me-Ade adenine derivatives in aqueous solution according to PCM/TD-DFT calculations employing different density functionals

| | PBE0 | LC-$\omega$PBE | CAM-B3LYP | M052X |
|---|---|---|---|---|
| 6-31$G(d)$ | | | | |
| S$n$ | 5.35 (0.00) | 5.52 (0.00) | 5.61 (0.00) | 5.67 (0.00) |
| $L_a$ | 5.18 (0.26) | 5.54 (0.33) | 5.43 (0.33) | 5.53 (0.36) |
| $L_b$ | 5.43 (0.07) | 5.60 (0.08) | 5.54 (0.04) | 5.66 (0.05) |
| 6-31+$G(d, p)$ | | | | |
| S$n$ | 5.35 (0.00) | 5.56 (0.00) | 5.63 (0.00) | 5.69 (0.00) |
| $L_a$ | 5.04 (0.31) | 5.37 (0.41) | 5.26 (0.38) | 5.37 (0.41) |
| $L_b$ | 5.32 (0.05) | 5.42 (0.02) | 5.45 (0.02) | 5.57 (0.03) |
| 6-311+$G(2d, 2p)$ | | | | |
| S$n$ | 5.33 (0.00) | 5.54 (0.00) | 5.61 (0.00) | 5.70 (0.00) |
| $L_a$ | 4.98 (0.30) | 5.31 (0.39) | 5.20 (0.37) | 5.31 (0.40) |
| $L_b$ | 5.26 (0.04) | 5.46 (0.02) | 5.39 (0.02) | 5.51 (0.03) |

The geometry optimized by each of the functionals (by using the 6-31$G(d)$ basis set) is used in the TD-DFT calculation. Oscillator strengths are given in parentheses

tion energies of their lowest energy transition, computing, for the first time, the absorption spectra of thymine and adenine nucleoside and nucleotide in aqueous solution. A methyl or a deoxyribose substituent on N1 of thymine leads to a small red-shift of the lowest energy bright electronic transition, and a relative stabilization of this state with respect to the close lying dark state. This latter result is also found for adenine and its derivatives. However, in aqueous solution the energy ordering of these two states does not change with the substituent on N1/N9, since solvent effects let the bright state be the lowest energy electronic state in the Franck–Condon region. Substituent effects could be more effective in a less polar environment or in the other regions of the potential energy surface, leading to a change of the energy ordering between the bright and the dark state. Since this result could significantly modulate the decay mechanism of the nucleobases [13,72], our study indicates that 1,methyl-thymine and 9,methyl-adenine are more suitable for modeling the behavior of the corresponding nucleosides and nucleotides than thymine and adenine. Ribose and phosphoribose substituents affect mainly the dark Sn transition of adenine and thymine, because of a significant mixing with the highest energy occupied non bonding orbital of purine and pyrimidine moieties, slightly increasing its oscillator strength. This result, while not affecting the absorption spectra, could modulate the excited state decay, since these states are believed to play some role in the deactivation mechanism [1,13]. Furthermore, from a dynamical point of view, important factors (such as, for example, vibrational cooling) are expected to be very different in nucleosides and nucleotides when compared to the simple nucleobases.

The present study allows also a first validation of different density functionals for the computation of nucleobases VEEs. The picture provided by PBE0 calculations is confirmed by the recently developed LC-$\omega$PBE, M052X and CAM-B3LYP density functionals. At least for what concerns the spectroscopic states, the first functional provides a VEE closer to the experimental band maximum. On the other hand, all the density functionals examined provide a similar description of the relative stability of the lowest energy (dark and bright) excited electronic states. This result paves the route for the application of the LC-$\omega$PBE, M052X and CAM-B3LYP functionals to the study of the nucleobase multimers, where a correct treatment of dispersion interactions and long-range CT electronic transitions could be very important.

**Acknowledgments** This paper is dedicated to Prof. Nino Russo for his 60th birthday. The authors thank Dr. Thomas Gustavsson and Dr. Fabrizio Santoro for very useful discussions, Gaussian Inc. for financial support, and Village-Na (http://village.unina.it) for computational resources.

## References

1. Crespo-Hernandez CE, Cohen B, Kohler B (2004) Chem Rev 104:1977
2. Wang CH (1985) Spectroscopy of condensed media. Academic Press, New York
3. Fleming GR (1986) Chemical applications of ultrafast spectroscopy. Oxford University, New York
4. Assion A, Baumert T, Bergt M, Brixner T, Kiefer B, Seyfried W, Strehle M, Gerber G (1998) Science 282:919
5. Crespo-Hernandez CE, Cohen B, Kohler B (2005) Nature 436:1141
6. Markovitsi D, Talbot F, Gustavsson T, Onidas D, Lazzarotto E, Marguet S (2006) Nature 441:E7

7. Markovitsi D, Onidas D, Gustavsson T, Talbot F, Lazzarotto E (2005) J Am Chem Soc 127:17130
8. Markovitsi D, Gustavsson T, Talbot F (2007) Photochem Photobiol Sci 6:717
9. Improta R, Barone V (2004) J Am Chem Soc 126:14320
10. Gustavsson T, Banyasz A, Lazzarotto E, Markovitsi D, Scalmani G, Frisch MJ, Barone V, Improta R (2006) J Am Chem Soc 128:607
11. Gustavsson T, Sarkar N, Lazzarotto E, Markovitsi D, Barone V, Improta R (2006) J Phys Chem B 110:12843
12. Gustavsson T, Sarkar N, Lazzarotto E, Markovitsi D, Improta R (2006) Chem Phys Lett 429:551–557
13. Santoro F, Barone V, Gustavsson T, Improta R (2006) J Am Chem Soc 128:16312
14. Matsika S (2004) J Phys Chem A 108:7584
15. Matsika S (2005) J Phys Chem A 109:7538
16. Zgierski MZ, Patchkovskii S, Fujiwara T, Lim EC (2005) J Phys Chem A 109:9384
17. Merchan M, Serrano-Andres L, Robb MA, Blancafort L (2005) J Am Chem Soc 127:1820
18. Zgierski MZ, Patchkovskii S, Lim EC (2005) J Chem Phys 123:081101
19. Marian CM (2005) J Chem Phys 122:104314
20. Marian C, Nolting D, Weinkauf R (2005) Phys Chem Chem Phys 7:3306
21. Nielsen SB, Slling TI (2005) Chem Phys Chem 6:1276
22. Sobolewski AL, Domcke W, Hattig C (2005) Proc Natl Acad Sci USA 102:17903
23. Perun S, Sobolewski AL, Domcke W (2005) J Am Chem Soc 127:6257
24. Blancafort L (2006) J Am Chem Soc 128:210
25. Serrano-Andres L, Merchan M, Borin AC (2006) Proc Natl Acad Sci 103:8691
26. Serrano-Andres L, Merchan M, Borin AC (2006) Chem Eur J 12:6559
27. Gustavsson T, Sharonov A, Markovitsi D (2002) Chem Phys Lett 351:195
28. Gustavsson T, Sharonov A, Onidas D, Markovitsi D (2002) Chem Phys Lett 356:49
29. Santoro F, Barone V, Improta R (2007) Proc Natl Acad Sci USA 104:9931
30. Cerný J, Spirko V, Mons M, Hobza P, Natchigallová D (2006) Phys Chem Chem Phys 8:3059
31. So R, Alavi S (2007) J Comput Chem 28:1776
32. Adamo C, Barone V (1999) J Chem Phys 110:6158
33. Adamo C, Barone V (1998) Chem Phys Lett 298:113
34. Improta R, Benzi C, Barone V (2001) J Am Chem Soc 123:12568
35. Improta R, Barone V, Kudin KN, Scuseria GE (2001) J Am Chem Soc 123:3311
36. Benzi C, Improta R, Scalmani G, Barone V (2002) J Comput Chem 23:341
37. Improta R, Mele F, Crescenzi O, Benzi C, Barone V (2002) J Am Chem Soc 124:7857
38. Langella E, Improta R, Barone V (2002) J Am Chem Soc 124:11531
39. Saracino GAA, Improta R, Barone V (2003) Chem Phys Lett 373:411
40. Adamo C, Scuseria G, Barone V (1999) J Chem Phys 111:2889
41. Guillemoles JF, Barone V, Joubert L, Adamo C (2002) J Phys Chem A 105:11354
42. Improta R, Santoro F, Dietl C, Papastathopoulos E, Gerber G (2004) Chem Phys Lett 387:509
43. Sanna N, Chillemi G, Grand A, Castelli S, Desideri A, Barone V (2005) J Am Chem Soc 127:15429
44. Wanko M, Garavelli M, Bernardi F, Niehaus TA, Frauenheim T, Elstner M (2004) J Chem Phys 120:1674
45. Tozer DJ, Amos RD, Handy NC, Roos BO, Serrano-Andres L (1999) Mol Phys 97:859
46. Dreuw A, Weisman JL, Head-Gordon M (2003) J Chem Phys 119:2943
47. Dreuw A, Head-Gordon M (2004) J Am Chem Soc 126:4007
48. Burke K, Werschnik J, Gross EKU (2005) J Chem Phys 123:62206
49. Gritsenko O, Baerends EJ (2004) J Chem Phys 121:655
50. Maitra NT, Zhang F, Cave RJ, Burke K (2004) J Chem Phys 120:5932
51. Maitra NT (2005) J Chem Phys 122:234104
52. Cai ZL, Crossley MJ, Reimers JR, Kobayashi R, Amos RD (2006) J Phys Chem B 110:15624
53. Kobayashi R, Amos RD (2006) Chem Phys Lett 420:106
54. Peach MJG, Helgaker T, Salek P, Keal TW, Lutnaes OB, Tozer DJ, Handy NC (2006) Phys Chem Chem Phys 8:558
55. Zheng JJ, Zhao Y, Truhlar DG (2007) J Phys Chem A 111:4632
56. Yanai T, Tew DP, Handy NC (2004) Chem Phys Lett 393:51
57. Vydrov OA, Scuseria GE (2006) J Chem Phys 125:234109
58. Zhao Y, Schultz NE, Truhlar DG (2006) J Chem Theory Comput 2:364
59. Levy M, Perdew JP (1993) Phys Rev B 48:11638
60. Lieb EH, Oxford S (1981) Int J Quantum Chem 19:427
61. Tawada Y, Tsuneda T, Yanagisawa S, Yanai T, Hirao K (2004) J Chem Phys 120:8425
62. Miertus S, Scrocco E, Tomasi J (1981) Chem Phys 55:117
63. Tomasi J, Mennucci B, Cammi R (2005) Chem Rev 105:2999
64. Cossi M, Barone V (2001) J Chem Phys 115:4708
65. Frisch MJ et al (2007) G03 Version, F.02. Gaussian Inc., Wallingford CT
66. Onidas D, Markovitsi D, Marguet S, Sharonov A, Gustavsson T (2002) J Phys Chem B 106:11367
67. Improta R, Barone V, Scalmani G, Frisch MJ (2006) J Chem Phys 125:54103
68. Improta R, Scalmani G, Frisch MJ, Barone V (2007) J Chem Phys 127:74504
69. Improta R, Barone V, Santoro F (2007) Angew Chemie Int Ed 46:405
70. Santoro F, Improta R, Lami A, Bloin J, Barone V (2007) J Chem Phys 126:84509
71. Santoro F, Lami A, Improta R, Barone V (2007) J Chem Phys 126:184102
72. Hare PM, Crespo-Hernandez C, Kohler B (2007) Proc Nat Acad Sci USA 104:435